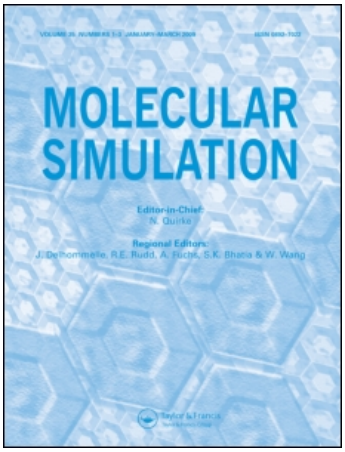

Molecular Simulation
Publication details, including instructions for authors and subscription information:
http://www.informaworld.com/smpp/title~content=t713644482

Molecular Dynamics Simulation of Silica Glass

B. Vessal[a]; M. Leslie[b]; C. R. A. Catlow[c]
[a] Department of Chemistry, University of Keele, Keele, UK [b] Daresbury Laboratory, Warrington, UK [c] Department of Chemsitry, University of Keele, Keele, UK

To cite this Article Vessal, B. , Leslie, M. and Catlow, C. R. A.(1989) 'Molecular Dynamics Simulation of Silica Glass', Molecular Simulation, 3: 1, 123 — 136
To link to this Article: DOI: 10.1080/08927028908034623
URL: http://dx.doi.org/10.1080/08927028908034623

Molecular Simulation, 1989, Vol. 3, pp. 123–136
Reprints available directly from the publisher
Photocopying permitted by license only

MOLECULAR DYNAMICS SIMULATION OF SILICA GLASS

B. VESSAL

Department of Chemistry, University of Keele, Keele, Staffs., ST5 5BG, UK.

M. LESLIE

Daresbury Laboratory, Warrington, WA4 4AD, UK.

and

C.R.A. CATLOW

Department of Chemsitry, University of Keele, Keele, Staffs, ST5 5BG, UK

(*Received May, 1988; in final form August 1988*)

To investigate the effects of angle bending terms on the structure of amorphous silica, three different potential models have been developed for the molecular dynamics simulation of vitreous silica.

KEY WORDS: Molecular dynamics, silica, vitreous, amorphous, glass, three body interactions.

I. INTRODUCTION

There have been several molecular dynamics (MD) simulation studies of vitreous silica [1–9] in the past few years. All of these simulations have been performed using simple Buckingham type short range potentials with no dispersion terms. Although they have been successful in predicting the radial distribution function (RDF) of glasses, there have been deficiencies in the results of calculations. This is particularly marked in the distribution of O–Si–O bond angles, which is far broader than that determined experimentally which finds a narrow distribution around the tetrahedral angle with a half width of one degree [10]. In this paper we report on the effects of modification of the interatomic potentials to include angle bending terms on the structure of simulated silica glass.

II. COMPUTATIONAL DETAILS

The molecular dynamics simulation is undertaken using a cubic simulation box measuring 21.48 Å on each side and containing 648 ions. Newton's equations of motion are integrated using Beeman's algorithm [11] and a timestep of 3.0×10^{-15}s. The glasses were prepared by melting a system of 648 ions of β-cristobalite contained in the simulation box at 10000 K and then cooling successively to 5000 K, 2500 K, 1200 K, and 293 K for seven and a half picoseconds, giving a total annealing time of thirty seven and a half picoseconds. The velocities were rescaled during the first 1000 timesteps at each temperature to equilibrate the system. The long range coulomb part

of the potential is computed using Ewald's method [12]. Following Sangster and Dixon [13], and Anastasiou and Fincham [14] we write the coulomb part of the potential as follows:

$$E^c = E_1^c + E_2^c + E_3^c \tag{1}$$

$$E_1^c = \sum_{\substack{i=1 \\ i>j}}^{N} \sum_{j=1}^{N} Z_i Z_j \frac{\mathrm{erfc}(\alpha r_{ij})}{r_{ij}} \tag{2}$$

$$E_2^c = -\sum_{i=1}^{N} Z_i^2 \alpha \pi^{-1/2} \tag{3}$$

$$E_3^c = \sum_{i=1}^{N} \sum_{\mathbf{k}\neq\mathbf{0}} \mathbf{A(k)}\, \mathbf{R}\left[\left(\sum_{j=1}^{N} Z_j e^{\mathbf{ik}.\mathbf{r}_j}\right) Z_i\, e^{-\mathbf{ik}.\mathbf{r}_i}\right] \tag{4}$$

where E_1^c and E_3^c are known as the direct and the reciprocal lattice parts of the coulomb energy respectively. N is the number of ions in the simulation box, Z_i and Z_j are the charges on ions i and j, r_{ij} is the distance between i and the nearest image of j, and α is called the Ewald parameter. The choice of this parameter determines the value of the direct and reciprocal sum cutoffs. If one wishes to determine the direct and reciprocal lattice sums to an accuracy A_c, then the value of the direct lattice cutoff that is used is $r_{max} = f/\alpha$, and the reciprocal lattice cutoff is $k_{max}/2\pi = \alpha f/\pi$, where $f = (-\ln A_c)^{1/2}$. We use a value of α that gives comparable numbers of terms in both the direct and reciprocal lattice sums i.e. [15].

$$\alpha = (N\pi^3/V^2)^{1/6} \tag{5}$$

where V is the volume of the simulation box. Symbol R is used to denote the real part of a complex quantity.

The sum over **k** need only be carried out over half of reciprocal space and the final result doubled since reciprocal space is always centrosymmetric. The z component of the reciprocal lattice vector will always be taken as positive.

In the above expression **k** is 2π times a reciprocal lattice vector, and **r** is an atom position. The maximum reciprocal lattice vectors in the x, y and z directions N_x, N_y, N_z are determined from the formula given below:

$$N_x = (k_{max}/2\pi)\,|\mathbf{l}_x|$$

where $\mathbf{l}_x$ is the x column of a matrix whose columns are the unit cell lattice vectors.

A(**k**) is defined as

$$\mathrm{A(k)} = 2\pi/\mathrm{V}\,\frac{\exp(-\mathrm{k}^2/4\alpha^2)}{\mathrm{k}^2} \tag{6}$$

A four range Buckingham potential is used to model the short range interactions between different ions.

$$E_{ij}^{SR} = A_{ij} \exp(-r_{ij}/\varrho_{ij}) \qquad r_{ij} < r_1 \tag{7}$$

$$E_{ij}^{SR} = A_1 r_{ij}^5 + B_1 r_{ij}^4 + C_1 r_{ij}^3 + D_1 r_{ij}^2 + E_1 r + F_1 \qquad r_1 < r_{ij} < r_2 \tag{8}$$

$$E_{ij}^{SR} = P_1 r_{ij}^3 + Q_1 r_{ij}^2 + R_1 r_{ij} + S_1 \qquad r_2 < r_{ij} < r_3 \tag{9}$$

$$E_{ij}^{SR} = -C_{ij}/r_{ij}^6 \qquad r_3 < r_{ij} < r_c \tag{10}$$

where r_c is the short range cutoff.

The function is splined at r_1, r_2 and r_3 to have continuous energy and first and second derivatives. The function has a minimum at r_2. The program was written with the CRAY XMP in mind. Although the short range potentials seem to be complicated, we are able to fit a cubic spline and use this in the forces calculation.

A cubic spline is either fitted separately to the coulomb direct space error function term and to the short range potential, or to the sum of the two terms. Two separate splines are needed if the pressure is required. One thousand points are used in the spline. The spline is fitted to the square of the distance to avoid calculating a square root. It should be noted that the forces calculation is still fully vectorisable on the XMP.

The "nearest image" convention [16] is used to calculate r_{ij}^2. This is tested against the square of the cutoff. The indices of all j within the cutoff of a given i ($j > i$) are sorted. This is a compress index loop on the XMP and is fully vectorisable. There is then a loop over these indices which calculates the force using the spline. This loop uses the gather/scatter hardware on the XMP both for the elements of the distance vector and for the coefficients of the spline. The loop is therefore fully vectorisable on the XMP.

An essential feature of our new potential model is the inclusion of two different types of three body potentials one between the O-Si-O triads and the other between Si–O–Si triads. Consider the three atoms i, j, and k interacting according to the following potential (see Figure 1)

$$E_{ijk} = 1/4\ A_{ijk} B_{ijk}^2 \exp(-r_{ij}/\varrho_1) \exp(-r_{ik}/\varrho_2) \tag{11}$$

where

$$A_{ijk} = k_{ijk}/2(\theta_o - \pi)^2 \tag{12}$$

$$B_{ijk} = (\theta_o - \pi)^2 - (\theta - \pi)^2 \tag{13}$$

k_{ijk} is the three body spring constant and θ_o is the equilibrium bond angle, i.e. 109° 28′ in the case of O–Si–O interactions and 144° for Si-O-Si interactions, and θ is the calculated bond angle.

As the framework is allowed to reconfigure its bonding during the simulation, we have to use a three-body potential which decays to zero at a chosen cutoff. The

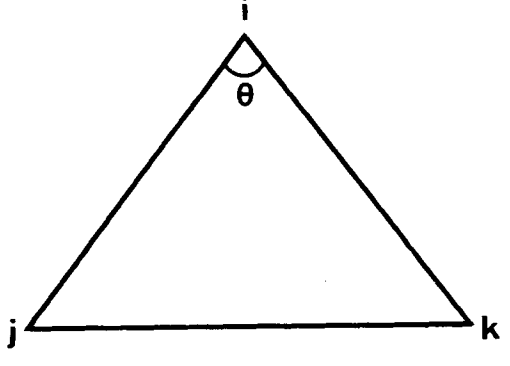

Figure 1 Schematic drawing of a triangle formed by three particles.

exponential part allows this to happen. The angle dependent part has the same energy and second derivative as a simple angle bending potential.

$$E_{ijk} = 1/2\, k_{ijk}\, (\theta - \theta_o)^2 \tag{14}$$

In order to be able to integrate the equations of motion using a relatively large timestep we had to use a large three body cutoff of 3.2 Å and a splined three body potential. Therefore we used equation (11) as our three body potential only if both r_{ij} and r_{ik} were less than 2.9 Å, otherwise if either r_{ij} or r_{ik} was greater than 2.9 Å and less than 3.2 Å then the relevant exponential term containing r_{ij} or r_{ik} was replaced by a fifth order polynomial in r_{ij^2} or r_{ik^2}. The parameters for the short range and three body potentials are determined using our THBFIT code which uses a least-squares fitting method to get the best agreement between the observed and the computed properties of α-quartz. We have fitted our potential parameters to those properties of α-quartz which are listed in Table II.

Table I lists the relevant parameters in the short range and the three body potentials. The observed and calculated properties of α-quartz based on our potential model are listed in Table II.

To calculate the forces due to the three body potential in the molecular dynamics code FUNGUS [17] and the crystal properties in the potential fitting program THBFIT, we need to determine the first and second derivatives of the potential with respect to the atomic coordinates. We use the same notation that was used before for the bond length derivatives [18].

$$F_s = 2\partial E_{ijk}/\partial(r_{ij}^2) \tag{15}$$

Table I Potential Parameters

Parameter	*Si–O Potential*		*O–O Potential*	
	Model I	Model II	Model I	Model II
A_{ij}/eV	1005.1563	788.5641	4978496.9000	22764.000
ϱ_{ij}/Å	0.3277	0.3563	0.149	0.149
C_{ij}/eVÅ^6)	25.00	0.0	52.12	27.88
k_{ijk}(Si–O–Si)/ (eV/radians^2)	0.0	3779.8		
k_{ijk}(O–Si–O)/ (eV/radians^2)	729.0189	37988.8		
A_1/(eV/Å^5)	−15.6911723	−17.7810115	−0.7894742	−0.2593615
B_1/(eV/Å^4)	−165.2261909	184.4365568	13.0952378	4.2341936
C_1/(eV/Å^3)	−697.1112644	−764.8054941	−86.6996290	−27.5357774
D_1/(eV/Å^2)	1484.1446300	1597.9533710	286.4412780	89.1613341
E_1/(eV/Å)	−1611.8417758	−1704.0948339	−472.3745705	−143.7588776
F_1/eV	724.2200617	754.9882648	311.1788448	92.3456341
P_1/(eV/Å^3)	−0.0233139	0.0	−0.0251198	−0.0134371
Q_1/(eV/Å^2)	0.2214821	0.0	0.3052061	0.1632606
R_1/(eV/Å)	−0.6702747	0.0	−1.2208242	−0.6530426
S_1/eV	0.6187898	0.0	1.5952103	0.8533090
r_1/Å	1.5	1.5	2.9	2.9
r_2/Å	2.5	2.5	3.6	3.6
r_3/Å	3.5	3.5	4.2	4.2
r_c/Å	7.6	7.6	7.6	7.6
ϱ_1/Å	0.3277	0.3563		
ϱ_2/Å	0.3277	0.3563		

Table II Observed and Calculated Properties of α-quartz

Experimental [23]		*Sanders Potential [20]*	*Model I*	*Model II*
Elastic constants (10^{11} dyn cm^{-2}) a)				
C_{11}	8.683	8.815	9.797	9.063
C_{33}	10.498	10.605	11.031	12.644
C_{44}	5.826	5.296	5.890	3.800
C_{66}	3.987	4.269	5.100	4.211
C_{14}	−1.806	−1.666	−1.361	−1.090
C_{13}	1.193	1.151	0.087	0.887
Static dielectric constants				
E_{11}	4.520	4.452	4.411	4.363
E_{33}	4.640	4.812	4.671	4.711

a) 1 dyn = 10^{-5}N

The corresponding derivatives with respect to r_{ik}^2 and r_{jk}^2 will be denoted by F_t and F_u respectively.

$$F_{ss} = 4\partial^2 E_{ijk}/\partial(r_{ij}^2)^2 \tag{16}$$

The derivatives with respect to $r_{ij}^2 r_{ik}^2$, $r_{ij}^2 r_{jk}^2$, $(r_{ik}^2)^2$, $r_{ik}^2 r_{jk}^2$, and $(r_{jk}^2)^2$ will be represented by F_{st}, F_{su}, F_{tt}, F_{tu} and F_{uu} respectively. For the three body potential in Equation (11)

$$F_s = A_{ijk} B_{ijk} \exp(-r_{ij}/\varrho_1) \exp(-r_{ik}/\varrho_2)(C_{ijk} G_s/\sin\theta - B_{ijk}/4r_{ij}\varrho_1) \tag{17}$$

where

$$G_s = \frac{1}{r_{ij} r_{ik}} - \frac{\cos\theta}{r_{ij}^2} \tag{18}$$

and

$$C_{ijk} = (\theta - \pi) \tag{19}$$

and

$$\begin{aligned} F_{ss} = {} & A_{ijk} \exp(-r_{ij}/\varrho_1) \exp(-r_{ik}/\varrho_2) \times \\ & \{G_s^2/\sin^2\theta\,(2C_{ijk}^2 - B_{ijk} + B_{ijk} C_{ijk} \cot\theta) + \\ & B_{ijk} C_{ijk}/\sin\theta\,[1/r_{ij}^3 r_{ik} - (3/r_{ij}^2 + 2/r_{ij}\varrho_1) G_s] + \\ & B_{ijk}^2/4r_{ij}\varrho_1\,[1/r_{ij}^2 + 1/r_{ij}\varrho_1]\} \end{aligned} \tag{20}$$

The remainder of the derivatives can be found in the Appendix. The first derivatives with respect to the atomic coordinates can be written as:

$$\partial E_{ijk}/\partial \mathbf{r}_i = \mathbf{r}_{ij} F_s + \mathbf{r}_{ik} F_t \tag{21}$$

and the second derivatives as:

$$\partial^2 E_{ijk}/\partial \mathbf{r}_i\, \partial \mathbf{r}_j = -\mathbf{R}_{ijik}^T + \mathbf{R}_{ijjk} + \mathbf{R}_{ikjk} - \mathbf{R}_{ijij} \tag{22}$$

where

$$\mathbf{R}_{ijik} = F_{st}\, \mathbf{r}_{ij} \cdot \mathbf{r}_{ik}^T \tag{23}$$

$$\mathbf{R}_{ijjk} = F_{su}\,\mathbf{r}_{ij}\cdot\mathbf{r}_{jk}^{T} \tag{24}$$

$$\mathbf{R}_{ikjk} = F_{tu}\,\mathbf{r}_{ik}\cdot\mathbf{r}_{jk}^{T} \tag{25}$$

$$\mathbf{R}_{ijij} = F_{ss}\,\mathbf{r}_{ij}\cdot\mathbf{r}_{ij}^{T} + F_{\wedge}\,\mathbf{I} \tag{26}$$

where $\mathbf{I}$ is the 3×3 identity matrix.

When θ approaches π the following two expressions in the derivatives are replaced by the proper power series in order to avoid getting indeterminate values for the derivatives.

$$\begin{aligned}
C_{ijk}/\sin\theta &= (\theta - \pi)/\sin\theta = -\frac{1}{\sin(\theta-\pi)}\{\sin^{-1}[\sin(\theta-\pi)]\} \\
&= -\frac{1}{\sin(\theta-\pi)}\{\sin(\theta-\pi) + \frac{\sin^3(\theta-\pi)}{6} \\
&\quad + 3/40\,\sin^5(\theta-\pi) \\
&= +5/112\,\sin^7(\theta-\pi) + \ldots] \\
&= -1 - 1/6\,\sin^2(\theta-\pi) - 3/40\,\sin^4(\theta-\pi) \\
&\quad - 5/112\,\sin^6(\theta-\pi)\ldots \\
(C_{ijk}/\tan\theta - 1)/\sin^2\theta &= \left(\frac{\theta-\pi}{\tan(\theta-\pi)} - 1\right)\Big/\tan^2\theta\cos^2\theta \\
&= \frac{1}{\tan(\theta-\pi)}\left\{\left[\tan(\theta-\pi) - \frac{\tan^3(\theta-\pi)}{3}\right.\right. \\
&\quad + \frac{\tan^5(\theta-\pi)}{5} \\
&\quad \left.\left. - \frac{\tan^7(\theta-\pi)}{7} + \ldots\right] - 1\right\}\Big/\tan^2\theta\cos^2\theta \\
&= \left[-\frac{\tan^2(\theta-\pi)}{3} + \frac{\tan^4(\theta-\pi)}{5} - \frac{\tan^6(\theta-\pi)}{7}\right. \\
&\quad \left. + \ldots\right]\Big/\tan^2(\theta-\pi)\cos^2(\theta-\pi) \\
&= 1/\cos^2(\theta-\pi)\left[-1/3 + \frac{\tan^2(\theta-\pi)}{5}\right. \\
&\quad \left. - \frac{\tan^4(\theta-\pi)}{7} + \ldots\right]
\end{aligned}$$

The coordination numbers and the bond angle distributions are calculated using a cutoff of 2.2 Å.

The pressure is determined using the following equation

$$\langle P\rangle = N/V\,k_B\langle T\rangle - \frac{1}{3V}\langle\psi\rangle \tag{27}$$

where the angular bracket represents a time average, k_B is Boltzman's constant, T is the temperature, and ψ is the total virial. The total virial is computed from the following equation [19]

$$\psi = -E^c + \sum_{\substack{i \\ i<j}} \sum_{j} (r_{ij}\, \partial\, E_{ij}^{SR}/\partial r_{ij}) + \sum_{\substack{i \\ i<j<k}} \sum_{j} \sum_{k} (r_{ij}\partial/\partial r_{ij} + r_{ik}\, \partial/\partial r_{ik} + r_{jk}\, \partial/\partial r_{jk})\, E_{ijk} \quad (28)$$

III RESULTS AND DISCUSSION

As mentioned earlier we have developed three different potential models for simulating vitreous silica, and for investigating the effect of three body forces on the structure of simulated glass. The experimental, and the computed properties of α-quartz using two of our potential models are listed in Table II. Also listed in Table II are the properties of α-quartz calculated using the potential model developed by Sanders, Leslie and Catlow [20].

If we compare the three potential models, bearing in mind that our potentials are rigid ion potentials while the potentials of Sanders *et al* are shell model ones, we can see that our potential models are quite satisfactory in predicting the observed properties of α-quartz.

The RDF, the coordination number, and the bond angle distributions (BAD) were calculated after running for six picoseconds at 293 K and were accumulated every ten timesteps for three hundred timesteps. We have started our simulation by modelling the structure of vitreous silica using our Model I potential. We can see from Table I that this model includes a three body interaction between the O–Si–O triads. We refer to the glass simulated using potential Model I as Glass I. Glass I has a pressure of about -50 kbar.

The RDF obtained for Glass I are compared with the X-ray results of Mozzi and Warren [21] in Table III. It can be seen that they agree well with the experiment. The BAD for Glass I are shown in Figs. 5–6. The O–Si–O BAD has a peak at 109° with a half width of 9°, while the O–Si–O BAD has a peak at 161°. This value is close to the experimentally derived value of 153° [22]. The coordination numbers for Glass I are listed in Table IV. It can be seen that about 89% of the silicons in Glass I are four

Table III Model I Structure

	First Peak	*Second Peak*
	g_{Si-O}	
Model I	1.62	4.12
Observed [21]	1.62	4.15
	g_{O-O}	
Model I	2.65	5.12
Observed [21]	2.65	5.1
	g_{Si-Si}	
Model I	3.2	5.1
Observed [21]	3.12	5.1

Table IV Coordination Numbers (as percent of total)

Coordination Number	*Glass I*	*Glass II*	*Glass III*
a — Silicon			
0	0	0	0.2
1	0	0.3	2.9
2	0.3	6.4	16.0
3	6.9	35.3	37.7
4	88.7	46.4	42.9
5	3.9	10.3	0.3
6	0.2	1.2	0
7	0	0.1	0
b — Oxygen			
0	0	0.3	0
1	3.9	26.6	42.7
2	93.8	64.0	54.1
3	2.3	9.0	3.2
4	0	0.1	0

coordinated while about 94% of the oxygens are two coordinated. To sharpen up the peak at 109° in the O–Si–O BAD we decided to develop a potential model which gave good crystal properties and contained stronger three body interactions. Also we wanted to shift the peak at 161° in the Si–O–Si BAD towards the experimental value of 153°. We hoped that we would be able to achieve this by including a three body term around the oxygens. Also we hoped that strengthening the three body interactions around the silicons and inclusion of a three body term around the oxygens would help to sharpen up the coordination numbers of silicons and oxygens respectively. That is why we have developed potential Model II. As can be seen from Table I the O–Si–O interactions are much stronger than those in Model I. This is achieved by increasing the three body forces around silicon at the expense of O–O repulsions. Glass II is the simulated glass that we get using our Model II potential and has a pressure of 90 kbar. The RDF for Glass II are plotted in Figures 2, 3, 4. It can be seen from these figures that the structure of Glass II is quite different from Glass I which compares well with experimental results. If we compare the Si–O RDF for Glass I and Glass II we can see that the RDF for Glass I has two peaks at 1.62 Å and 2.2 Å, while Glass II has two peaks at 1.55 Å and 2.2 Å. We have examined the geometry of SiO_4 units in both Glass I and Glass II. In Glass I only 8% of all the tetrahedra have three short bonds ($\sim$ 1.62 Å) and a long bond ($\sim$ 2.2 Å) while 92% of SiO_4 units have four short bonds. In Figure 1 if i is a Si atom and j and k are both oxygen atoms, and we take both the Si–O distances to be 1.62 Å and the O–O distance to be 2.65 Å (from the first peak in O-O RDF for Glass I), then the value of θ will be 109.75° which is close to the tetrahedral angle and corresponds to the peak in BAD for Glass I. If one of the Si–O distances is taken to be 2.2 Å then the value of θ will be 86.45° which corresponds to the shoulder in BAD for Glass I. In Glass II the percentage of four coordinated silicons are much smaller (see Table IV). Of all the SiO_4 units in Glass II 26% have four short bonds ($\sim$ 1.55 Å), 52% have three short Si–O bonds and one long ($\sim$ 2.2 Å) Si–O bond, while 22% have two short and two long Si–O bonds. If both of the Si–O bond lengths are 2.2 Å and the O–O bond length is taken to be 2.67 Å (from the first peak in O–O RDF for Glass II) the O–Si–O bond angle will be 74.72° which corresponds to the first shoulder in BAD for Glass II.

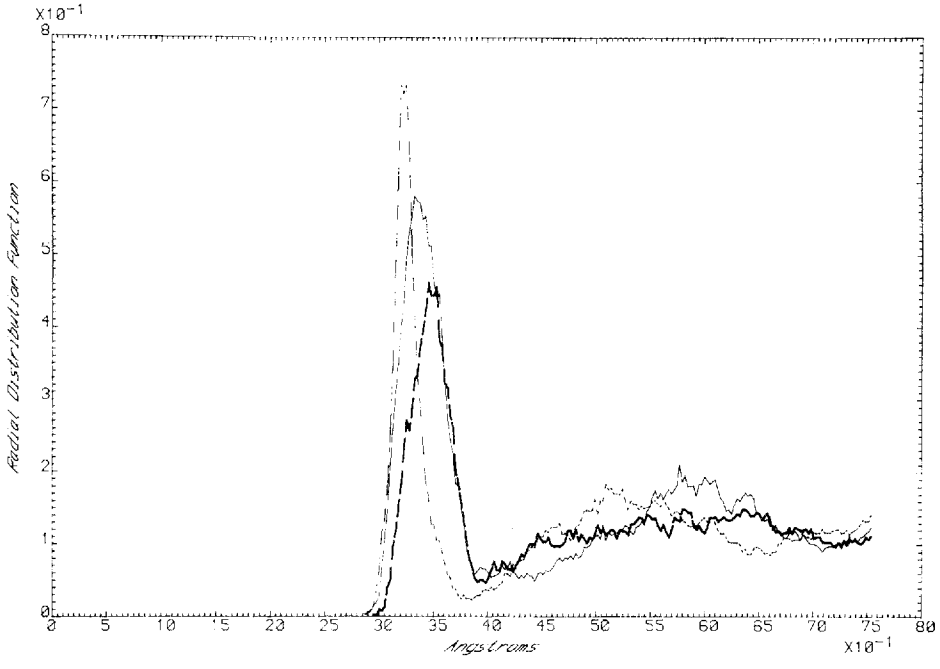

Figure 2 Si–Si RDF, Glass I (dashed line), Glass II (solid line), Glass III (heavy dashed line).

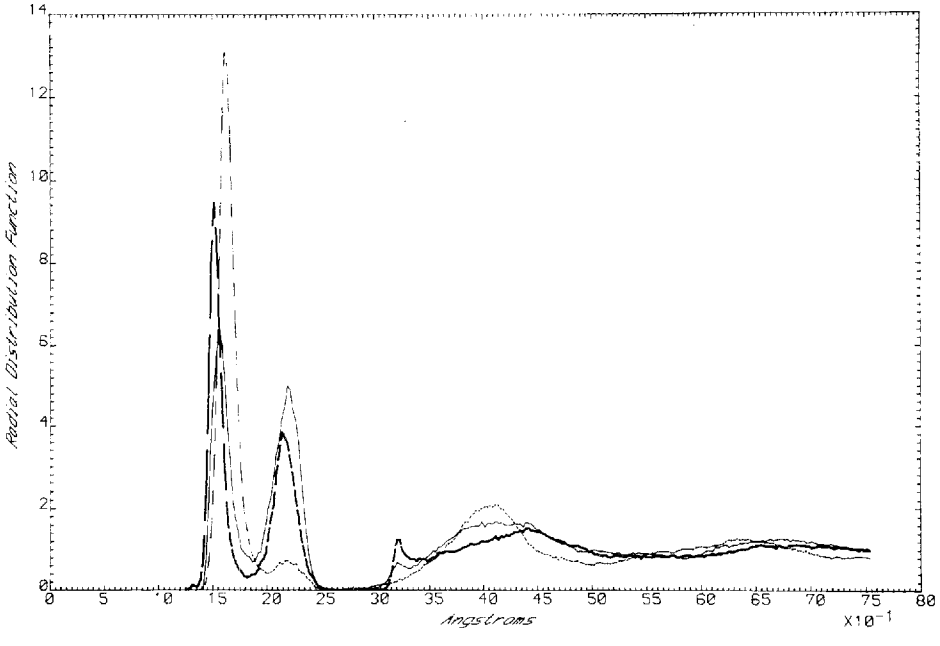

Figure 3 Si–O RDF, Glass I (dashed line), Glass II (solid line), Glass III (heavy dashed line).

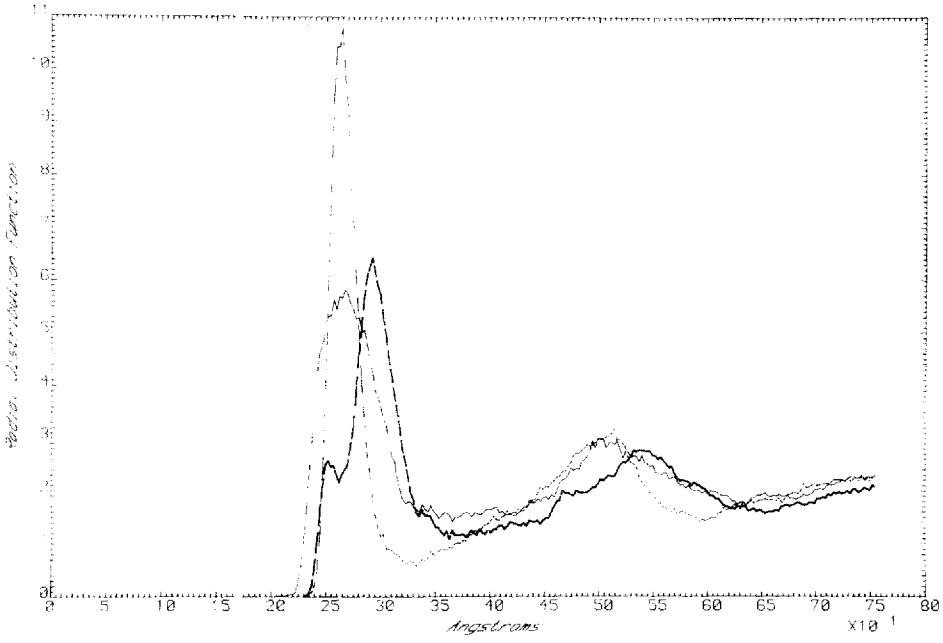

Figure 4 O–O RDF. Glass I (dashed line), Glass II (solid line), Glass III (heavy dashed line).

Of all the five coordinated Si atoms in Glass I 42% have four short Si–O bonds and a long Si–O bond, 52% have three short Si–O and two long Si–O bonds, and only 6% have two short Si–O bonds and three long Si–O bonds.

The SiO_6 units in Glass I have the following geometries: 73% have three short Si–O bonds, and three long Si–O bonds, while the rest have two short Si–O bonds and four long Si–O bonds.

The five coordinated silicons in Glass II have the following geometries: 2% have four short Si–O bonds and one long Si–O bonds and one long Si–O bond, 44% have two short Si–O bonds and three long Si–O bonds, while 54% have three short Si–O bonds and two long Si–O bonds. Of all the six coordinated silicons 11% have one short Si–O bond and five long Si–O bonds, 67% have two short Si–O bonds and four long Si–O bonds, while 22% have three short and three long Si–O bonds. The seven coordinated silicons in Glass II have the following geometries: 46% have two short and five long bonds, 46% have one short and six long bonds while 8% have three short and four long bonds.

Since we did not achieve our goal by developing our potential Model II, we decided to see the effect of the three body forces directly on the structure of silica glass by modifying our potential Model II.

All of the parameters in our third potential model are the same as those of Model II except the O–Si–O, and the Si–O–Si three body spring constants which are adjusted to 200000 and 8000 eV/radian^2 respectively. Glass III is the glass that we have simulated using our potential Model III and has a pressure of 185 kbar. If we look at Figs. 2–5 we see that there are two peaks in the Si–O RDF for Glass III at 1.5 and 2.15 Å respecitively. Also there are two peaks in the O–O RDF for Glass III at 2.52

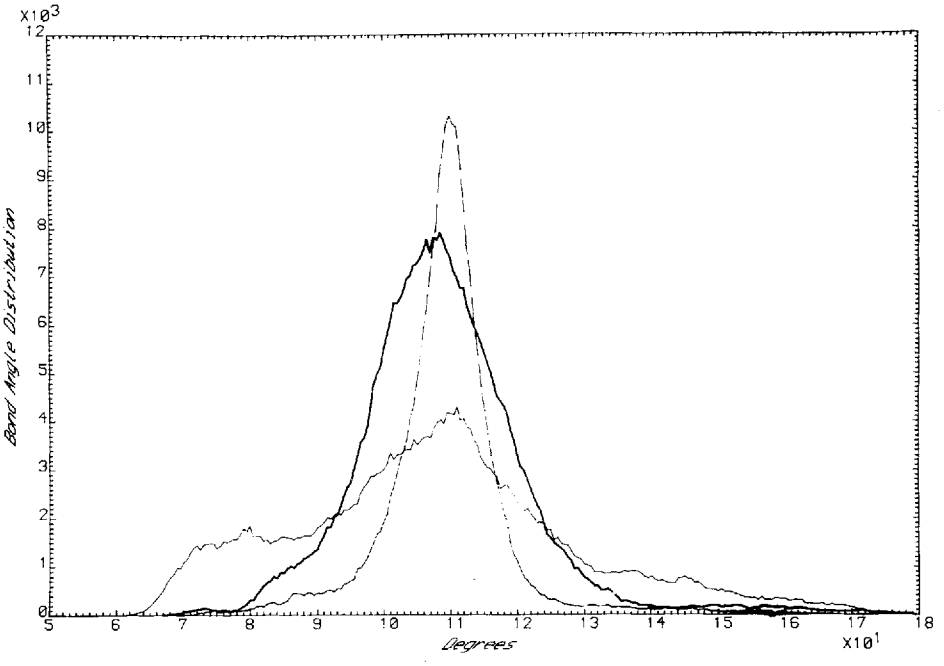

Figure 5 O–Si BAD, Glass I (heavy solid line), Glass II (solid line), Glass III (dashed line).

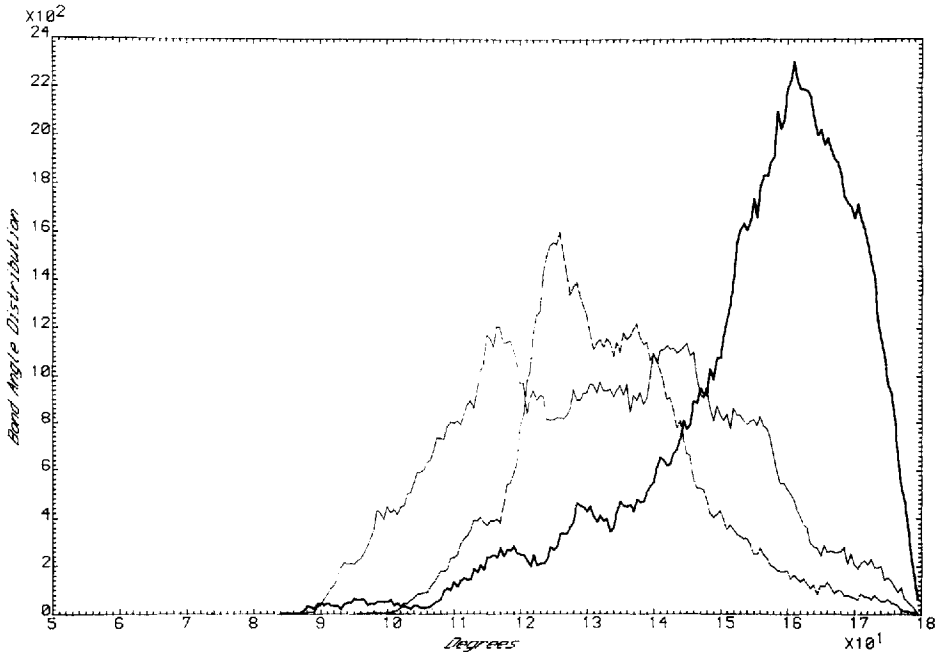

Figure 6 Si–O–Si BAD, Glass I (heavy solid line), Glass II (solid line), Glass III (dashed line).

and 2.92 Å respectively while the Si–Si RDF for Glass III has a peak at 3.45 Å. The O–Si–O BAD for Glass III is quite sharp and has a half width of only 5 degrees, as can be seen from Figure 5. The Si–O–Si BAD for Glass III has a peak at 126° and a shoulder at 137° (Figure 6). If in Figure 1 i is a Si atom and j and k are two oxygen atoms then the geometries that give angles corresponding to those seen in Figure 5 are the following: a) If both the Si–O bonds are taken to be 1.5Å and the O–O bond is taken to be 2.52 Å then θ will be 114.28°. b) if one Si–O bond is taken to be 1.5 Å while the other is taken to be 2.15 Å, and the O–O bond is taken to be 2.92 Å then θ is calculated to be 104.86°.

In case of the Si–O–Si bond angle if one Si–O bond length is taken to be 1.5 Å and the other is taken to be 2.15 Å and the Si–Si bond length is taken to be 3.45 Å then θ is calculated to be 141.25°.

Analysis of the geometry of SiO_4 and SiO_5 units in Glass III proves this. Of all the four coordinated Si atoms in Glass III 52% have three short Si–O bonds and one long bond, 45% have two short Si–O bonds and two long bonds while only 3% have four short Si–O bonds. Of all the five coordinated silicons 47% have two short Si–O bonds and three long bonds while 53% have one short Si–O bond and four long bonds.

CONCLUSIONS

Of the three potential models that we have developed for simulation of vitreous silica Model I gives structures that compare well with the experiment. Comparing Model II and Model III shows the effect of the three body forces on the bond angles and sharpening of the BAD. Our potential Model I is the first potential model to our knowledge that gives good crystalline properties and reasonable glass structure for SiO_2.

Acknowledgements

We thank Dr. W. Smith and Dr. J.M. Parker for fruitful discussions, and Mrs. H. Hitchen for typing the manuscript.

Appendix

Here is a list of the bond length derivatives which were not given in the text.

$$G_t = \frac{1}{r_{ij}\, r_{ik}} - \frac{\cos\theta}{r_{ik}^2}$$

$$G_u = -\frac{1}{r_{ij}\, r_{ik}}$$

$$F_t = A_{ijk}\, B_{ijk} \exp(-r_{ij}/\varrho_1) \exp(-r_{ik}/\varrho_2) \left(\frac{C_{ijk}\, G_t}{\sin\theta} - \frac{B_{ijk}}{4 r_{ik}\, \varrho_2}\right)$$

$$F_u = A_{ijk} B_{ijk} \exp(-r_{ij}/\varrho_1) \exp(-r_{ik}/\varrho_2) \left(\frac{C_{ijk}\, G_u}{\sin\theta}\right)$$

$$F_{st} = A_{ijk} \exp(-r_{ij}/\varrho_1) \exp(-r_{ik}/\varrho_2) \left\{ \frac{G_s G_t}{\sin^2\theta} (2C^2{}_{ijk} - B_{ijk} + B_{ijk} C_{ijk} \cot\theta - \frac{B_{ijk} C_{ijk}}{\sin^2\theta} \left[\frac{\cos\theta}{r_{ij}^2 r_{ik}^2} + \left(\frac{1}{r_{ik}^2} + \frac{1}{r_{ik}\varrho_2} \right) G_s + \left(\frac{1}{r_{ij}\varrho_1} \right) G_t \right] + \frac{B_{ijk}^2}{4 r_{ij}\varrho_1} \left(\frac{1}{r_{ik}\varrho_2} \right) \right\}$$

$$F_{su} = A_{ijk} \exp(-r_{ij}/\varrho_1) \exp(-r_{ik}/\varrho_2) \left\{ \frac{G_s G_u}{\sin^2\theta} (2C_{ijk}^2 - B_{ijk} + B_{ijk} C_{ijk} \cot\theta) + + \frac{B_{ijk} C_{ijk}}{\sin\theta} \left[\frac{1}{r_{ij}^3 r_{ik}} - \left(\frac{1}{r_{ij}\varrho_1} \right) G_u \right] \right\}$$

$$F_{tt} = A_{ijk} \exp(-r_{ij}/\varrho_1) \exp(-r_{ik}/\varrho_2) \times \left\{ \frac{G_t^2}{\sin^2\theta} (2C_{ijk}^2 - B_{ijk} + B_{ijk} C_{ijk} \cot\theta) + + \frac{B_{ijk} C_{ijk}}{\sin\theta} \left[\frac{1}{r_{ik}^3 r_{ij}} - \left(\frac{3}{r_{ik}^2} + \frac{2}{r_{ik}\varrho_2} \right) G_t \right] + \frac{B_{ijk}^2}{4 r_{ik}\varrho_2} \left(\frac{1}{r_{ik}^2} + \frac{1}{r_{ik}\varrho_2} \right) \right\}$$

$$F_{tu} = A_{ijk} \exp(-r_{ij}/\varrho_1) \exp(-r_{ik}/\varrho_2) \times \left\{ \frac{G_t G_u}{\sin^2\theta} (2C_{ijk}^2 - B_{ijk} + B_{ijk} C_{ijk} \cot\theta) + + \frac{B_{ijk} C_{ijk}}{\sin\theta} \left[\frac{1}{r_{ik}^3 r_{ij}} - \left(\frac{1}{r_{ik}\varrho_2} \right) G_u \right] \right\}$$

$$F_{uu} = A_{ijk} \exp(-r_{ij}/\varrho_1) \exp(-r_{ik}/\varrho_2) \times \left[\frac{G_u^2}{\sin^2\theta} (2 C_{ijk}^2 - B_{ijk} + B_{ijk} C_{ijk} \cot\theta) \right]$$

References

[1] L.V. Woodcock, C.A. Angell and P. Cheeseman, "Molecular dynamics studies of the vitreous state: Simple ionic systems and silica", *J. Chem. Phys.*, **65**,1565 (1976).

[2] T.F. Soules, "A molecular dynamic calculation of the structure of sodium silicate glasses", ibid, 71, 4570 (1979).

[3] S.K. Mitra and R.W. Hockney, "Distribution of holes in simulated silicon dioxide glass", *J. Phys. C.*,**13**, L739 (1980).

[4] S.K. Mitra, M. Amini, D. Fincham and R.W. Hockney, "Molecular dynamics simulation of silicon dioxide glass", *Phil. Mag. B*, **43**, 365 (1981).

[5] S.H. Garofalini, "Molecular dynamics simulation of the frequency spectrum of amorphous silica", *J. Chem. Phys.*, **76**, 3189 (1982).

[6] S.K. Mitra, "Molecular dynamics simulation of silicon dioxide glass", *Phil. Mag. B*, **45**, 529 (1982).

[7] S.H. Garofalini, "Pressure variation in molecular dynamics simulated vitreous silica", *J. Non-Crystalline Solids*, **55**, 451 (1983).

[8] S.K. Mitra, "Constant-pressure simulation of silica", *Phil. Mag. B*, **47**, L63 (1983).

[9] S.H. Garofalini, "Defect species in vitreous silica — A molecular dynamics simulation", *J. Non-Crystalline Solids*, **63**, 337 (1984).

[10] D.L. Griscom, E.J. Friebele, G.H. Sigel, Jr. and R.J. Ginther, "Radiation-induced paramagnetic defects as structural probes of pure silica and borosilicate glasses", *The Structure of Non-Crystalline Materials*,edited by P.H. Gaskell (London: Taylor and Francis Ltd), 113 (1977).

[11] D. Beeman, "Some multistep methods for use in molecular dynamics calculations", *J. Comp. Phys.*, **20**, 130 (1976).

[12] P. Ewald, "Die Berechnung optischer und elektrostatischer Gitterpotentiale", *Ann. Physik*, **64**, 253 (1921).

[13] M.J.L. Sangster and M. Dixon, "Interionic potentials in alkali halides and their use in simulations of the molten salts", *Advances in Physics*, **25**, 247 (1976).

[14] N. Anastasiou and D. Fincham, "Programs for the dynamic simulation of liquids and solids," *Comput. Phys. Commun.*, **25**, 159 (1982).
[15] C.R.A. Catlow and W.C. Mackrodt, Computer Simulation of Solids. Lecture Notes in Physics Vol. 166, edited by C.R.A. Catlow and W.C. Mackrdot (Berlin: Springer-Verlag), 3 (1982).
[16] D. Fincham and D.M. Heyes, "Recent advances in molecular dynamics computer simulation", *Advances in Chem. Phys., LXIII*, **493** (1985).
[17] J.R. Walker, Computer Simulation of Solids. Lecture Notes in Physics Vol. 166, edited by C.R.A. Catlow and W.C. Mackrodt (Berlin: Springer-Verlag), 65 (1982).
[18] M. Leslie, "First and second derivatives of three body force terms for ionic crystal calculations", Daresbury Laboratory Technical Memorandum No. DL/SCI/TM36T, (1984).
[19] R. Vogelsang and C. Hoheisel, "Comparison of various potential models for the simulation of the pressure of liquid and fluid N_2", *Phys. Chem. Liq.*, **16**, 189 (1987).
[20] M.J. Sanders, M. Leslie and C.R.A. Catlow, "Interatomic potentials for SiO_2", *J. Chem. Soc., Chem. Commun.*, 1271 (1984).
[21] R.L. Mozzi and B.E. Warren, "The structure of vitreous silica", *J. Applied Crys.*, **2**, 164 (1969).
[22] J.R.G. Da Silva, D.G. Pinatti, C.E. Anderson and M.L. Rudee, "A refinement of the structure of vitreous silica", *Phil. Mag.*, **31**, 713 (1975).
[23] I. Koga, M. Aruga, and Y. Yoshinaka, "Theory of plane elastic waves in a piezoelectric crystalline medium and determination of elastic and piezoelectric constants of quartz", *Phys. Rev.*, **109**, 1467 (1958).